

# Superradiant Solid in Cavity QED Coupled to a Lattice of Rydberg Gas

Xue-Feng Zhang,<sup>1</sup> Qing Sun,<sup>2</sup> Yu-Chuan Wen,<sup>3</sup> Wu-Ming Liu,<sup>2</sup> Sebastian Eggert,<sup>1</sup> and An-Chun Ji<sup>3,\*</sup>

<sup>1</sup>*Physics Department and Research Center OPTIMAS,  
University of Kaiserslautern, 67663 Kaiserslautern, Germany*

<sup>2</sup>*Institute of Physics, Chinese Academy of Sciences, Beijing 100190, China*

<sup>3</sup>*Department of Physics, Capital Normal University, Beijing 100048, China*

(Dated: October 13, 2018)

We study an optical cavity coupled to a lattice of Rydberg atoms, which can be represented by a generalized Dicke model. We show that the competition between the atomic interaction and atom-light coupling induces a rich phase diagram. A novel “superradiant solid” (SRS) phase is found, where both the superradiance and crystalline orders coexist. Different from the normal second order superradiance (SR) transition, here both the Solid-1/2 and SRS to SR phase transitions are first order. These results are confirmed by the large scale quantum Monte Carlo simulations.

PACS numbers: 42.50.Pq, 03.75.Nt, 05.30.Jp, 67.10.Fj

*Introduction.*— The study of quantum many-body problems and quantum phase transitions (QPT) has attracted great interest and is currently one of the main issues in the condensed matter community [1]. In the past decade, the successful control of the interaction strength and dimensionality of ultracold quantum gases has made it possible to explore many interesting physical phenomena [2]. For example, the observation of the superfluid-Mott insulator transition [3], a Tonks gas [4], the BEC to BCS crossover [5], and the Kosterlitz-Thouless phase transition [6] have all been established in ultra-cold quantum gases.

More recently ultracold atoms have been combined with cavity QED [7, 8] to study atom-light coupled many-body problems, which give rise to new phenomena. In particular, when the two-level atom gas is coupled to a cavity [9] the coherent non-local atom-light interaction supports the famous superradiance (SR) phase transition in the Dicke model (DM) [10, 11]. This SR phase is formed by the condensation of atom-light coupled polaritons [12] and breaks the U(1) symmetry. However, the interactions between atoms, which may bring new phenomena or induce novel QPTs, are not considered in the DM.

Atomic interactions promise to give interesting new effects and can be implemented via Rydberg atoms. The unique properties of strong dipole-dipole interactions and quite long lifetimes have made them a powerful tool for the implementation of coherent blockade effects and quantum information [13]. Especially, the successful trapping of Rydberg atoms in a 1D optical lattice [14] has stimulated the study of many-body quantum systems such as spin system [15, 16] and dynamical crystallization or melting of ultracold atoms [17, 18].

In this Letter, we now analyze the generalized DM by coupling a 1D lattice of Rydberg atoms with an optical cavity, where the dipole interaction between two Rydberg atoms competes with the atom-light coupling. We see that, while the atom-light interaction favors the SR

phase, the atomic interaction tends to form three incompressible Rydberg solid states with filling numbers 0, 1/2, and 1, which destroys the polariton formation. Most importantly, we find a novel state corresponding to a “superradiant solid” (SRS) phase, where both the superradiance and crystalline orders coexist and the corresponding U(1) and translation symmetries are broken simultaneously. Compared with the supersolid (SS) phase in an optical lattice [19–21], which breaks the same symmetries, the SRS is rather unique as it is induced by the non-local atom-light coupling and the condensation of polaritons. Moreover we find that, while the Solid-(0, 1) to SR phase transitions remain second order, both the Solid-1/2 and SRS to SR phase transitions become first order.

*The model.*— The system consists of a deep 1D lattice with  $N$  sites in an optical cavity. Each site is occupied by a single atom with the ground state  $|g\rangle$  coupled to a high-lying Rydberg state  $|e\rangle$  via a two-photon transition process [22]. The Hamiltonian of this system in the rotating-wave approximation is given by

$$\begin{aligned} \hat{H} = & \omega \psi^\dagger \psi + \sum_{i=1}^N \frac{\epsilon}{2} (b_i^\dagger b_i - a_i^\dagger a_i) + \frac{g}{\sqrt{N}} \sum_{i=1}^N (b_i^\dagger a_i \psi + \text{H.c.}) \\ & + C_6 \sum_{\langle i,j \rangle} P_{ee}^{(i)} P_{ee}^{(j)} - \mu N_{\text{ex}}, \end{aligned} \quad (1)$$

where  $\omega$  and  $\epsilon$  are the cavity and atom transition frequencies with the detuning defined by  $\Delta = \omega - \epsilon$ .  $\psi^\dagger$  is the single-mode creation operator of the cavity field,  $a_i$  and  $b_i$  are the boson operators representing the lower and upper levels of each atom and satisfy the single-occupancy constraint  $b_i^\dagger b_i + a_i^\dagger a_i = 1$  and  $g_{\text{eff}} \equiv g/\sqrt{N}$  is the effective two-photon coupling. The strong dipole-dipole interactions  $C_6$  between two Rydberg states is modeled by projectors  $P_{ee}^{(i)} = n_i \equiv b_i^\dagger b_i$  onto the Rydberg state, where only nearest interactions are considered [15]. The last term is the chemical potential for the total number of excitations  $N_{\text{ex}} = \psi^\dagger \psi + \sum_{i=1}^N b_i^\dagger b_i$ .

The above model possesses two limiting cases. First for

$C_6 = 0$ , the Hamiltonian (1) becomes the DM. Here we note that, because the ground state  $|g\rangle$  of the atoms is not directly coupled to the Rydberg state  $|e\rangle$ , the so called no-go theorem [23] does not apply [24], and the SR phase can occur. Recently, the SR phase transition has been observed with a superfluid atomic gas in an optical cavity [9]. Secondly, when  $g$  is zero this system becomes a pure lattice of Rydberg atoms. Then by tuning the chemical potential  $\tilde{\mu} \equiv \mu - \omega$ , one may derive three Rydberg solid states: (i)  $\tilde{\mu} < -\Delta$ , it forms a Solid-0 phase with all the atoms staying in the ground state; (ii)  $-\Delta < \tilde{\mu} < 2C_6 - \Delta$ , half of the atoms are excited to the Rydberg states and form a Solid-1/2 phase because of the nearest neighbor repulsion; (iii)  $\tilde{\mu} > 2C_6 - \Delta$ , all the atoms are excited to the Rydberg states forming a Solid-1 phase.

*Analytical Approach.*—A convenient starting point is to consider the limit  $g \ll C_6$ . In this case, one may take the atom-light interaction as a perturbation and use the strong coupling expansion (SCE) [25]. By comparing the energies of exciting a particle or hole with the correction from second order processes in the solid phase, we derive the following melting critical lines of the incompressible solid lobes [26]:

$$\begin{aligned} \text{Solid-0:} & \quad \tilde{\mu}_{c1} = -\Delta - g^2/\Delta, \\ \text{Solid-1/2:} & \quad \tilde{\mu}_{c2} = -\Delta + g^2/(2\Delta), \\ & \quad \tilde{\mu}_{c3} = -\Delta + 2C_6 - g^2/(2\Delta - 4C_6), \\ \text{Solid-1:} & \quad \tilde{\mu}_{c4} = -\Delta + g^2/(\Delta - 2C_6) + 2C_6, \\ & \quad \tilde{\mu}_{c5} = -g^2/(\Delta - 2C_6), \end{aligned}$$

which are shown as dashed lines in Fig. 2. The melting will make the solid compressible, but it needs to be explored if the order in the Solid-1/2 state is actually destroyed or may be stable even in the presence of particle or hole excitations.

For this purpose we introduce a variational ground wavefunction [12] to gain a more physical insight into the phase diagram:

$$|\lambda, \theta\rangle = \exp\left(\frac{\lambda\sqrt{N}\psi^\dagger}{2}\right) \prod_i [\cos\left(\frac{\theta_i}{2}\right)b_i^\dagger + \sin\left(\frac{\theta_i}{2}\right)a_i^\dagger]|0\rangle, \quad (2)$$

where  $|0\rangle$  denotes the vacuum state with all atoms in the ground state, and  $\lambda$  and  $\theta_i$  are the variational parameters for the coherent cavity field and atomic fields. To find the ground state, we calculate the energy density  $\mathcal{E} \equiv 4\langle\lambda, \theta|H|\mathcal{V}|\lambda, \theta\rangle/N$ :

$$\begin{aligned} \mathcal{E} = & \quad 4[-g\lambda(\sin\theta_A + \sin\theta_B) + C_6 \cos\theta_A \cos\theta_B \\ & \quad -\tilde{\mu}\lambda^2 - (\tilde{\mu} + \Delta - C_6)(\cos\theta_A + \cos\theta_B)], \quad (3) \end{aligned}$$

where we have assumed two sublattices  $A$  and  $B$ . From Eq. (3) we see that while the  $g$ -term tends to enhance the cavity field  $\lambda$  and the condensation of polaritons, the second  $C_6$ -term favors the staggered order of the polaritons. After minimizing  $\mathcal{E}$  in respect to the variational parameters, we derive the phase diagram Fig. 1. The corresponding variational values are shown in TABLE I, where the

solid phases represent the Rydberg crystals without coherent cavity excitations. The usual superradiance phase is denoted by SR, where the atoms and light form polaritons and condense with a nonzero order parameter  $\langle b_i^\dagger a_i \rangle = \sin\theta_{\text{SR}}/2$  and a coherent cavity field  $\lambda_{\text{SR}}$ . The

Variational values	Solid-0	SRS	SR	Solid-1/2	Solid-1
$\theta_A$	$\pi$	$\theta_1$	$\theta_{\text{SR}}$	0	0
$\theta_B$	$\pi$	$\theta_2$	$\theta_{\text{SR}}$	$\pi$	0
$\lambda$	0	$\lambda_{\text{SRS}}$	$\lambda_{\text{SR}}$	0	0

TABLE I: The variational values for different phases, where  $\theta_1 \neq \theta_2$  in SRS phase.

most interesting finding is that, when  $g \sim C_6$  there exists an intermediate SRS phase between the Solid-1/2 and SR phases. Different from the SR phase where the polaritons are excited uniformly, the SRS phase also breaks the translation symmetry, which shows a characteristic excitation density  $\rho_{A,B} = (\cos\theta_{1,2} + 1)/2$  that is not equal on the two sublattices. Therefore, both the superradiance and crystalline orders coexist in the SRS phase. In Fig. 1, we also see that the solid lobes shrink with decreasing  $\Delta$ .

In bipartite lattices with nearest neighbor repulsion of bosons a related supersolid (SS) phase is known to exist, but this phase is only stable for *soft-core* contact interaction in a 1D Bose-Hubbard (BH) model [21]. It is therefore surprising to find an SRS phase in our system which is effectively described by hard-core bosons, since only a single polariton can be excited in each site. Here we note that, different from the BH model, there is no direct kinetic hopping term but instead the non-local cavity field couples with all atoms simultaneously. This is the unique property that makes the appearance of the SRS rather nontrivial in this system.

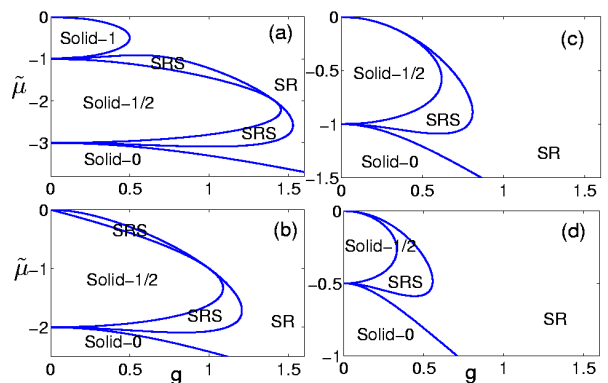


FIG. 1: Variational phase diagram for (a)  $\Delta = 3$ , (b)  $\Delta = 2$ , (c)  $\Delta = 1$ , and (d)  $\Delta = 0.5$ . All parameters are in units of  $C_6$ .

However, the above results are derived from mean-field calculations, so the SRS phase may not be stable when quantum effects are taken into account. In particular,

when a particle (or hole) is introduced into the Solid-1/2 phase, the strong quantum fluctuation of the non-local atom-cavity coupling may drive the particle (or hole) to move freely on the whole lattice, which may destroy the staggered solid order and drive the Solid-1/2 phase directly into the SR phase. Another possibility is that the SRS phase may be unstable and separates into domains [20]. To settle these issues and demonstrate explicitly the phase diagram, one needs an unbiased numerical simulation to go beyond mean-field theory.

*Quantum Monte Carlo (QMC) simulations.*—We adopt the high-accuracy cluster Stochastic Series Expansion algorithm [28, 29]. This algorithm is very efficient and has no truncation error arising from the limitation of the photon number. In order to distinguish different phases, one needs to calculate several observables: the average excitation density  $\rho = \langle N_{\text{ex}} \rangle / N$ , the structure factor  $S(q)/N = \langle |\sum_{k=1}^N n_k e^{iqr_k}|^2 \rangle / N^2$ , and the compressibility  $\kappa = N\beta(\langle \rho^2 \rangle - \langle \rho \rangle^2)$ . For the half filled Solid-1/2 phase, we take the structure factor  $S(Q)/N$  with staggered order  $Q = \pi$  to characterize the translational symmetry breaking.

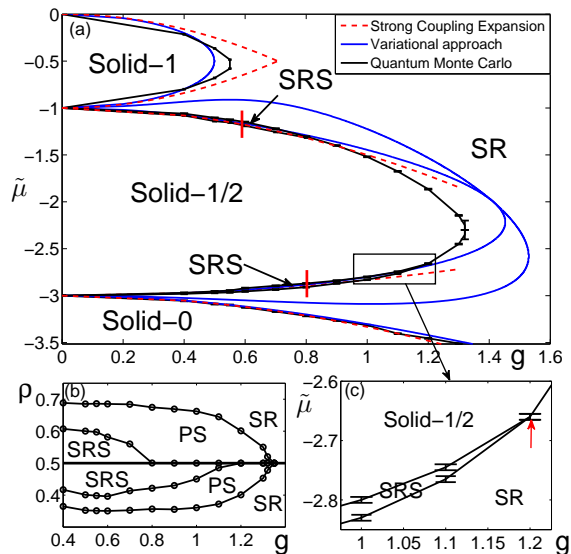


FIG. 2: (color online). (a) The phase diagram obtained by different methods for  $C_6 = 1$  and  $\Delta = 3$  in the grand-canonical ensemble. (b) The phase diagram obtained by QMC in the canonical ensemble. Here, PS denotes the phase separation between the Solid-1/2, SRS and SR phase transitions. (c) The enlarged region of the SRS phase, where the red arrow marks the tricritical point among SRS, SR and Solid-1/2 phases.

Fig. 2(a) shows the zero-temperature phase diagram for  $\Delta = 3$  and  $C_6 = 1$ , where the dashed lines of SCE match quite well with the QMC calculations. Compared with the mean-field results the SRS phase is greatly suppressed, indicating that quantum fluctuations weaken the SRS order. Nonetheless, the SRS phase remains stable

in a small region as shown in the enlarged region of the SRS phase in Fig. 2(c). In first sight it appears difficult to reach such narrow regions of the SRS phase experimentally. However, this changes when considering the phase diagram in the canonical ensemble in Fig. 2(b), where the SRS phase exists in a wide region  $\Delta\rho \approx 0.1$  in the excitation density. In Fig. 2(b) we also find that the region of the particle-excited SRS phase is smaller than the hole-excited one. The phase separated (PS) regions show that both the Solid-1/2 and the SRS to SR phase transitions are first order. This differs from the mean-field results and may be understood by the Ginzburg Landau theory [27]: Because the U(1) and translation symmetries are broken simultaneously, the corresponding order parameters  $S(Q)/N$  and  $\langle b_i^\dagger a_i \rangle$  couple to each other and contribute to a sixth-order term in the free energy, which results in the first order phase transition. Moreover, a tricritical point appears among the SRS, SR and Solid-1/2 phases, see Fig. 2(c).

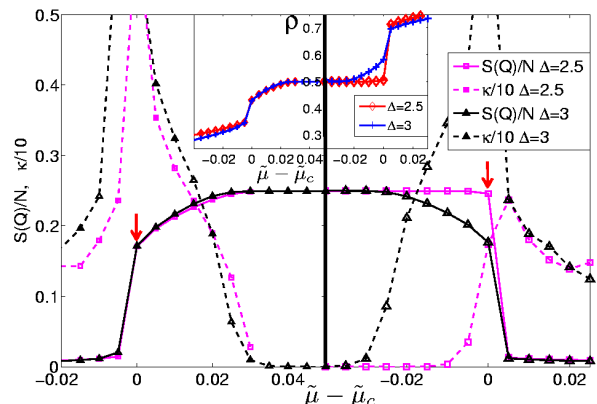


FIG. 3: (color online). The structure factor  $S(Q)/N$  (solid line) and compressibility  $\kappa/10$  (dash line) along the trajectories of the lower (left panel) and upper (right panel) vertical cuts indicated by solid bars in Fig. 2(a). Here, the red arrows mark the critical points with  $\tilde{\mu} = \tilde{\mu}_c$ . For all cases  $C_6 = 1$ ,  $\beta = 500$ ,  $N = 100$ , and  $\Delta = 3$  ( $\Delta = 2.5$ ). The inset shows the corresponding average excitation density  $\rho$ . For simplicity, the small errorbars for the observables are not shown here.

To provide a convincing support for the above phase diagram, we now concentrate on the detailed properties of the phase transitions. Figure 3 shows  $S(Q)/N$  and  $\kappa/10$  along the trajectories which are indicated by solid vertical lines (red) in Fig. 2(a). Here, we take  $T = C_6/500$ , which is low enough to avoid the thermal effect. In both panels, there exist regions where a vanishing structure factor  $S(Q)/N \rightarrow 0$  is accompanied by a finite  $\kappa$ , which means that the translational symmetry is not broken and they are compressible, which is characteristic of the SR phases. Regions of zero  $\kappa$  with finite  $S(Q)/N$  correspond to the incompressible Solid-1/2 phases. Most significantly, there exist intermediate SRS phases which have

both finite  $S(Q)/N$  and  $\kappa$ . The corresponding structure factor  $S(Q)/N$  and average density excitation  $\rho$  have a finite jump and  $\kappa$  diverges on the critical points  $\tilde{\mu} = \tilde{\mu}_c$ . It signifies that the SR to SRS phase transition is first order. In Fig. 3, we also show the results for different  $\Delta$ . We find that, while the region of the SRS phase in the left panel is hardly affected by  $\Delta$ , the one in the right panel shrinks faster by decreasing  $\Delta$ . This can be understood by the second-order atom-light interaction process which differs for a particle or hole excited state with corresponding second-order energies  $E_p^{(2)} \sim -\frac{g^2}{(\Delta-2C_6)}$  and  $E_h^{(2)} \sim -\frac{g^2}{\Delta}$ , respectively. Note that  $|E_p^{(2)}| > |E_h^{(2)}|$ , which means the particle excited SRS phase is harder to form than the hole excited one and more easily suppressed by decreasing  $\Delta$ .

We have also made a finite size scaling analysis for points in the SRS phase to demonstrate that the existence of the SRS phase is robust in the thermodynamic limit. Figure 4 shows the corresponding scaling results in the SRS phase. We see that both  $S(Q)/N$  and  $\kappa$  converge to finite values in the infinite size limit.

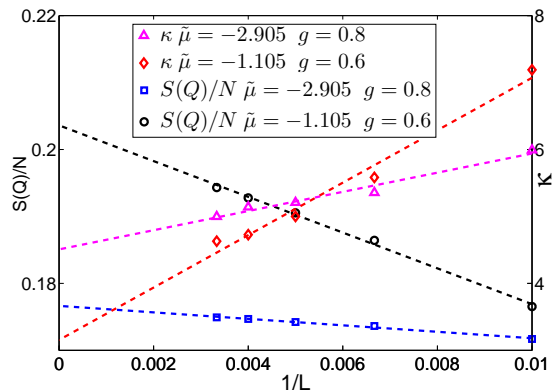


FIG. 4: (color online). The finite size scaling for  $S(Q)/N$  and  $\kappa$  at  $C_6 = 1$ ,  $\Delta = 3$  and  $\beta = 500$  vs different sizes.  $\tilde{\mu} = -2.905$  ( $-1.105$ ) correspond to the SRS phases on the trajectories of the lower (upper) cuts shown in Fig. 2(a).

*Discussion.*—Finally, we discuss two issues about the experimental implementation. First, this system could potentially be realized by trapping a lattice of  $^{87}\text{Rb}$  atoms coupled to an ultrahigh finesse cavity [22]. The  $5S_{1/2}$  ground atomic state can be coupled to the  $50D_{5/2}$  Rydberg excitation state [14] through a two-photon process via the  $5P_{3/2}$  intermediate state, which can be adiabatically eliminated. The resulting effective coupling constant  $g_{\text{eff}}$  is of order 10 MHz, which is higher than both the decay rates of the cavity and the Rydberg state. Secondly, we have assumed in the model that only a single Rydberg excitation is possible per site. Actually, this does not imply only one atom per site, but instead one may work with the collective degree of freedom of multiple atoms on each site, where only a single Rydberg state

can be excited and shared among all the atoms [18].

*Conclusion.*—We have shown that the generalized Dicke model of a cavity QED coupled with a Rydberg lattice gas displays a rich phase diagram. The competition between the non-local atom-light coupling and the atomic interaction can stabilize a novel SRS phase. By implementing an unbiased QMC calculation, we find that both the Solid-1/2 and SRS to SR phase transitions are first order, and the hole-excited SRS phase is more stable than the particle-excited one. This system may act as a new quantum simulator for the future study of quantum many-body physics.

We acknowledge Tao Wang for helpful discussions. This work is supported by NCET, NSFC under grants No. 11704175, 10904096, NSFB under grants No.1092009, NKBRSCF under grants No. 2011CB921502 and by the DFG via the SFB/Transregio 49.

\* Electronic address: [andrewjee@sina.com](mailto:andrewjee@sina.com)

- [1] S. Sachdev, *Quantum Phase Transitions* (Cambridge University Press, Cambridge, 1999).
- [2] I. Bloch, J. Dalibard, and W. Zwerger, *Rev. Mod. Phys.* **80**, 885 (2008); I. Bloch, J. Dalibard, and S. Nascimbéne, *Nature Phys.* **8**, 267 (2012).
- [3] M. Greiner, M. O. Mandel, T. Esslinger, T. Hänsch, and I. Bloch, *Nature* **415**, 39 (2002).
- [4] B. Paredes *et al.*, *Nature* **429**, 277 (2004); T. Kinoshita, T. Wenger, and D. S. Weiss, *Science* **305**, 1125 (2004).
- [5] Q. J. Chen, J. Stajic, S. N. Tan, and K. Levin, *Phys. Rep.* **412**, 1 (2005).
- [6] Z. Hadzibabic, P. Krüer, M. Cheneau, B. Battelier, and J. Dalibard, *Nature* **441**, 1118(2006).
- [7] F. Brennecke, T. Donner, S. Ritter, T. Bourde, M. Köhl, and T. Esslinger, *Nature* **450**, 268 (2007).
- [8] Y. Colombe, T. Steinmetz, G. Dubois, F. Linke, D. Hunger, and J. Reichel, *Nature* **450**, 272 (2007).
- [9] K. Baumann, C. Guerlin, F. Brennecke, and T. Esslinger, *Nature* **464**, 1301 (2010).
- [10] R. H. Dicke, *Phys. Rev.* **93**, 99 (1954).
- [11] K. Hepp and E. H. Lieb, *Ann. Phys. (N.Y.)* **76**, 360 (1973).
- [12] P. R. Eastham and P. B. Littlewood, *Phys. Rev. B* **64**, 235101 (2001).
- [13] For a review, see M. Saffman, T. G. Walker, and K. Mølmer, *Rev. Mod. Phys.* **82**, 2313 (2010) and references therein.
- [14] S. E. Anderson, K. C. Younge, and G. Raithel, *Phys. Rev. Lett.* **107**, 263001 (2011).
- [15] B. Olmos, R. González-Férez, and I. Lesanovsky, *Phys. Rev. Lett.* **103**, 185302 (2009).
- [16] I. Lesanovsky, *Phys. Rev. Lett.* **106**, 025301 (2011).
- [17] T. Pohl, E. Demler, and M. D. Lukin, *Phys. Rev. Lett.* **104**, 043002 (2010).
- [18] H. Weimer and H. P. Büchler, *Phys. Rev. Lett.* **105**, 230403 (2010).
- [19] P. Sengupta, L. P. Pryadko, F. Alet, M. Troyer, and G. Schmid, *Phys. Rev. Lett.* **94**, 207202 (2005).

- [20] S. Wessel and M. Troyer, Phys. Rev. Lett. **95**, 127205 (2005).
- [21] G. G. Batrouni, F. Hébert, and R. T. Scalettar, Phys. Rev. Lett. **97**, 087209 (2006).
- [22] C. Guerlin, E. Brion, T. Esslinger, and K. Molmer, Phys. Rev. A **82**, 053832 (2010).
- [23] K. Rzażewski, K. Wódkiewicz, and W. Żakowicz, Phys. Rev. Lett. **35**, 432 (1975); I. Białynicki-Birula and K. Rzażewski, Phys. Rev. A **19**, 301 (1979).
- [24] J. Larson and M. Lewenstein, New J. Phys. **11**, 063027 (2009).
- [25] J. K. Freericks, H. Monien, Phys. Rev. B **53**, 2691 (1996).
- [26] Details of the SCE calculation will be shown elsewhere.
- [27] X. F. Zhang, R. Dillenschneider, Y. Yu and S. Eggert, Phys. Rev. B **84**, 174515 (2011).
- [28] A. W. Sandvik, Phys. Rev. B **59**, R14157 (1999).
- [29] K. Louis and C. Gros, Phys. Rev. B **70**, 100410 (2004).